

## **Acknowledgements**

This dissertation was performed at the Vietnam Auger Training Laboratory (VATLY) located in the premises of the Institute for Nuclear Science and Technology under the supervision of Prof. Pierre Darriulat. During the time working in the laboratory I really enjoyed the friendly and open working environment that he had created there. On this occasion, I would like to express my heartfelt and deep gratitude to him for supervising me with enthusiasm and teaching me a lot of things in both science and life.

I also thank all VATLY members, particularly MSc Pham Thi Tuyet Nhung, for their help. They gave me a lot of useful advice and share their experience with me when I worked in the lab.

I am thankful to Dr Nguyen Quynh Lan and other professors who had taught me during the past four years when I was their student in the Faculty of Physics of Hanoi University of Education.

I would like also to thank all the friends in my class Y9, Faculty of Physics, Hanoi University of Education for their encouragement and help.

Finally, I am very grateful to my parents for having brought me up and having done their utmost to help me with my studies.

Hanoi, 10 / 5 / 2009

Do Thi Hoai

# 1. Introduction

The capture of a member of a binary star by a massive star or black hole, the other member being ejected, is an important phenomenon in dense environments [1] such as the centres of galaxies or of globular clusters. Its study implies solving the three-body problem, a notoriously difficult problem in Newton's dynamics. The purpose of this dissertation is to study the phenomenon using a simple computer simulation.

In the following section we describe the main properties of binary stars, and in particular of X-ray binaries. A third section gives a brief description of the centre of the Milky Way with emphasis on X-ray binaries as revelators of a large abundance of stellar black holes. The fourth section is a brief reminder about the three-body problem. The fifth section describes the computer simulation used in the present code and uses as a test bench the two body case where Kepler's laws apply. The sixth section studies the three body case and describes under which conditions capture occurs and which is the associated cross section. Conclusions and a short summary are given at the end.

## 2. Binary stars

### 2.1. Generalities on binary stars



Figure 1: Hubble image of the Sirius binary system, in which Sirius B can be clearly distinguished (lower left)

A binary star is a star system consisting of two stars orbiting around their common center of mass. The brighter star is called the primary and the other is its companion star or secondary. Many stars are part of either binary star systems or star systems with more than two stars, called multiple star systems. The term double star may be used synonymously with binary star, but more generally, a double star may be either a binary star or an optical double star which consists of two stars

with no physical connection appearing close together in the sky as seen from the Earth. A double star may be determined to be optical if its components have sufficiently different proper motions or radial velocities, or if parallax measurements reveal its two components to be at sufficiently different distances from the Earth. Binary star systems are very important in astrophysics because calculations of their orbits allow the masses of their component stars to be directly determined, which in turn allows other stellar parameters, such as radius and density, to be indirectly estimated. This also determines an empirical mass-luminosity relationship (MLR) from which the masses of single stars can be estimated.

Binary stars are often detected optically, in which case they are called *visual binaries*. They may also be detected by indirect techniques, such as

spectroscopy (*spectroscopic binaries*) or astrometry (*astrometric binaries*). If a binary star happens to orbit in a plane along our line of sight, its components will mutually eclipse and transit each other; these pairs are called eclipsing *binaries*, or, as they are detected by their changes in brightness during eclipses and transits, *photometric binaries*.

If the orbits of components in binary star systems are close enough they can gravitationally distort their mutual outer stellar atmospheres. In some cases, these *close binary systems* can exchange mass, which may bring their evolution to stages that single stars cannot attain. Famous examples of binaries are Algol (an eclipsing binary), Sirius (of which one member is a white dwarf) and Cygnus X-1 (of which one member is a black hole). Recently, it was shown that the stellar activity observed in globular clusters, notoriously composed of old stars and not expected to show any sign of stellar activity, was indeed due to close binary systems inducing a resurrection of stellar activity in the cluster.

It is estimated that approximately  $1/3$  of the star systems in the Milky Way are binary or multiple, with the remaining  $2/3$  consisting of single stars. There is a direct correlation between the period of revolution of a binary star and the eccentricity of its orbit, with systems of short period having smaller eccentricity. Binary stars may be found with any conceivable separation, from pairs orbiting so closely that they are practically in contact with each other, to pairs so distantly separated that their connection is indicated only by their common proper motion through space.

Because a large proportion of stars exist in binary systems, binaries are particularly important to our understanding of the processes by which stars form. In particular, the period and masses of the binary tell us about the amount of angular momentum in the system. Because this is a conserved

quantity in physics, binaries give us important clues about the conditions under which the stars were formed.

## ***2.2. Formation of Binaries***

Qualitatively, it is not surprising that a gas cloud, which has originally a very complex shape and structure, prefers to contract into two or more ultimately spherical stars than in a single one. Quantitatively, however, it turns out to be very difficult to describe the condensation process. It is only very recently, with the availability of powerful computers and simulation codes, that progress has been achieved. The direct fragmentation of protostellar gas clouds may occur in early phases of collapse (at cloud densities  $\sim 10^3 - 10^{10} \text{ cm}^{-3}$ ). But at higher densities, clouds are unable to cool efficiently upon contraction. In such cases, direct fission of rapidly rotating protostars seems to be a more likely mechanism.

If protostellar objects are assumed to be self-gravitating, incompressible fluids with uniform vorticity, one can show analytically that their allowed equilibrium configurations are defined by spheroids or ellipsoids. As they contract, conserving angular momentum and mass, their evolution may proceed through progressively flatter configurations and, if one follows evolution along a more and more distorted ellipsoidal sequence, one finds that eventually other configurations, with even higher order surface distortions, become energetically favorable. For example, there is a “dumbbell-binary sequence” that branches smoothly off the ellipsoid sequence.

One might imagine, therefore, that binary stars form from the slow contraction of a rapidly rotating gas cloud via the dumbbell-binary sequence. In reality, however, the picture is not that simple. In particular, it was shown recently that realistic fission models must incorporate a significant degree of differential rotation. Yet, it seems clear that a wide variety of rapidly rotating,

non axi-symmetric systems can be constructed with compressible equations of state, giving confidence that fission offers a viable route to binary star formation.

### ***2.3. History***

Since the invention of the telescope, many pairs of double stars have been found. Early examples include Mizar and Acrux. Mizar, in the Big Dipper (Ursa Major), was observed to be double by Giovanni Battista Riccioli in 1650 (and probably earlier by Benedetto Castelli and Galileo). The bright southern star Acrux, in the Southern Cross, was discovered to be double by Father Fontenay in 1685.

John Michell was first to suggest that double stars might be physically attached to each other when he argued in 1767 that the probability that a double star was due to a chance alignment was small. William Herschel began observing double stars in 1779 and soon thereafter published catalogs of about 700 double stars. By 1803, he had observed changes in the relative positions in a number of double stars over the course of 25 years, and concluded that they must be binary systems; the first orbit of a binary star, however, was not computed until 1827, when Félix Savary computed the orbit of  $\xi$  Ursae Majoris. Since this time, many more double stars have been catalogued and measured. The Washington Double Star Catalog, a database of visual double stars compiled by the United States Naval Observatory, contains over 100,000 pairs of double stars, including optical doubles as well as binary stars. Orbits are known for only a few thousand of these double stars.

## 2.4. Classification

A *visual binary* star is a binary star for which the angular separation between the two components is great enough to permit them to be observed as a double star in a telescope. The resolving power of the telescope is an important factor in the detection of visual binaries, and as telescopes become larger and more powerful an increasing number of visual binaries are detected. The brightness of the two stars is also an important factor, as brighter stars are harder to separate due to their glare than dimmer ones are.



Figure 2: The two components of Albireo, a typical visual binary.

Sometimes, the only evidence of a binary star comes from the Doppler effect on its emitted light. In these cases, the binary consists of a pair of stars where the spectral lines in the light from each one shifts first toward the blue, then toward the red, as each moves first toward us, and then away from us, during its motion about their common center of mass, with the period of their common orbit. In these systems, the separation between the stars is usually very small, and the orbital velocity very high. Unless the plane of the orbit happens to be perpendicular to the line of sight, the orbital velocities have components in the line of sight and the observed radial velocity of the system varies periodically. Since radial velocity can be measured with a spectrometer by observing the Doppler shift of the star spectral lines, the binaries detected in this manner are known as *spectroscopic binaries*. Most of these cannot be

resolved as a visual binary, even with telescopes of the highest existing resolving power.

An *eclipsing binary star* is a binary star in which the orbit plane of the two stars lies so nearly in the line of sight of the observer that the components undergo mutual eclipses. In the case where the binary is also a spectroscopic binary and the parallax of the system is known, the binary is quite valuable for stellar analysis. In the last decade, measurement of eclipsing binaries fundamental parameters has become possible with 8 meter class telescopes. This makes it feasible to use them as standard candles. Recently, they have been used to give direct distance estimates to the LMC, SMC, Andromeda Galaxy and Triangulum Galaxy. Eclipsing binaries offer a direct method to gauge the distance to galaxies to a new improved 5% level of accuracy. Eclipsing binaries are variable stars, not because the light of the individual components varies but because of the eclipses. The light curve of an eclipsing binary is characterized by periods of practically constant light, with periodic drops in intensity. If one of the stars is larger than the other, one will be obscured by a total eclipse while the other will be obscured by an annular eclipse.

Astronomers have discovered some stars that seemingly orbit around an empty space. *Astrometric binaries* are relatively nearby stars which can be seen to wobble around a point in space, with no visible companion. The same mathematics used for ordinary binaries can be applied to infer the mass of the missing companion. The companion could be very dim, so that it is currently undetectable or masked by the glare of its primary; or it could be an object that emits little or no electromagnetic radiation, such as a black hole or neutron star. If the companion is sufficiently massive to cause an observable shift in position of the star, then its presence can be deduced.



Another classification is based on the distance of the stars, relative to their sizes: *Detached binaries* are binary stars where each component is within its Roche lobe, i.e. the area where the gravitational pull of the star itself is larger than that of the other component. The stars have no major effect on each other, and essentially evolve separately. Most binaries belong to this class. *Semidetached binary stars* are binary stars where one of the components fills the binary star's Roche lobe and the other does not. Gas from the surface of the Roche lobe filling component (donor) is transferred to the other, accreting star. The mass transfer dominates the evolution of the system. In many cases, the inflowing gas forms an accretion disc around the accretor. A *contact binary* is a type of binary star in which both components of the binary fill their Roche lobes. The uppermost part of the stellar atmospheres forms a *common envelope* that surrounds both stars. As the friction of the envelope brakes the orbital motion, the stars may eventually merge.

Finally, it is possible for widely separated binaries to lose gravitational contact with each other during their lifetime as a result of external perturbations such as a. close encounter between two binary systems or between a binary and a more massive object (as we shall study below). The components, or at least one of them, may then move on to evolve as single stars. One then speaks of runaway stars.

### ***2.5. Strongly interacting binaries***

When a binary system contains a compact object such as a white dwarf, neutron star or black hole, gas from the other, donor, star can accrete onto the compact object. This releases gravitational potential energy, causing the gas to become hotter and emit radiation. Cataclysmic variables, where the compact object is a white dwarf, are examples of such systems. In X-ray binaries, the compact object can be either a neutron star or a black hole. These

binaries are classified as low-mass or high-mass according to the mass of the donor star. High-mass X-ray binaries contain a young, early type, high-mass donor star which transfers mass by its stellar wind, while low-mass X-ray binaries are semidetached binaries in which gas from a late-type donor star overflows the Roche lobe and falls towards the neutron star or black hole. Probably the best known example of an X-ray binary at present is the high-mass X-ray binary Cygnus X-1. In Cygnus X-1, the mass of the unseen companion is believed to be about nine times that of our Sun and is believed to be a black hole.

As a main sequence star increases in size during its evolution, it may at some point exceed its Roche lobe, meaning that some of its matter ventures into a region where the gravitational pull of its companion star is larger than its own. The result is that matter will transfer from one star to another through a process known as Roche Lobe overflow (RLOF), either being absorbed by direct impact or through an accretion disc. The mathematical point through which this transfer happens is called the first Lagrangian point. It is not uncommon that the accretion disc is the brightest (and thus sometimes the only visible) element of a binary star.

If a star grows outside of its Roche lobe too fast for all abundant matter to be transferred to the other component, it is also possible that matter will leave the system through other Lagrange points or as stellar wind, thus being effectively lost to both components. Since the evolution of a star is determined by its mass, the process influences the evolution of both companions, and creates stages that can not be attained by single stars.

If a white dwarf has a close companion star that overflows its Roche lobe, the white dwarf will steadily accrete gases from the star's outer atmosphere. These are compacted on the white dwarf's surface by its intense

gravity, compressed and heated to very high temperatures as additional material is drawn in. The white dwarf consists of degenerate matter, and so is largely unresponsive to heat, while the accreted hydrogen is not. Hydrogen fusion can occur in a stable manner on the surface through the CNO cycle, causing the enormous amount of energy liberated by this process to blow the remaining gases away from the white dwarf's surface. The result is an extremely bright outburst of light, known as a nova. In extreme cases this event can cause the white dwarf to exceed the Chandrasekhar limit and trigger a supernova that destroys the entire star.

## 2.6. X ray binaries

Since the late 60's, there have been many scientific satellites whose mission has been to detect and investigate the X-ray emission of celestial objects. As X-rays cannot propagate through the atmosphere, satellites are necessary to detect them.

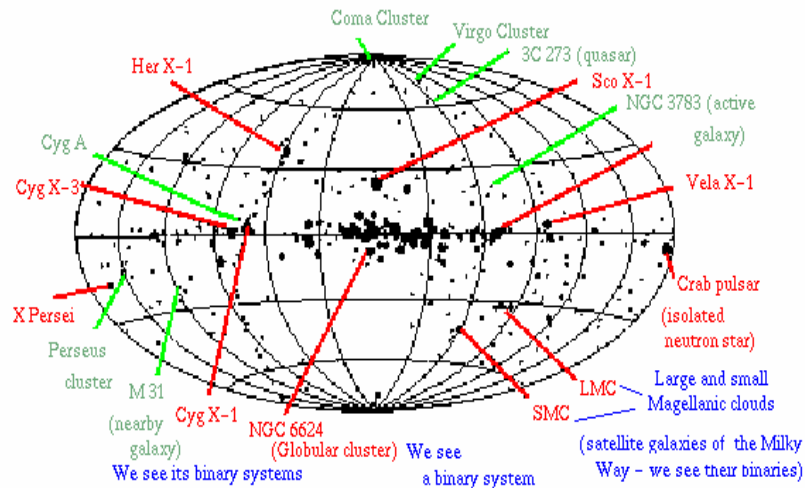


Figure 3: The all-sky map generated by *Uhuru* is shown in galactic coordinates (relative to the plane of our Galaxy). Most X-ray sources are on the galactic plane. A few selected objects are named. Sources which are not at all associated with our Galaxy are marked in green. Galactic sources are in red.

One of the first satellites dedicated to the study of X-rays was *Uhuru*. It produced a map of the strongest X-ray sources in the sky. Most of the sources were observed to be inside the Milky Way. Their energy output could be as high as several  $10^{38}$  ergs/s. “Normal” stars were sufficiently well known to be sure that they could not produce such X-rays. It was necessary to find a physical explanation for the presence of these point-like high-energy sources. The only possible mechanism for generating the radiation is the gravitational acceleration of particles in the gravitational field of compact objects.

Compact objects are the result of stellar evolution and are made of extremely dense matter. There are three kinds of compact objects: white dwarfs, neutron stars and black holes. The gravitational fields of these objects are enormous. Material falling towards these objects is accelerated to relativistic velocities and then stopped in some kind of collision on or close to the surface of the compact object. Its energy is then liberated in the form of X-rays. Most X-ray sources correspond to binary systems in which the compact object is dragging material from its companion. They are called X ray binaries. There are many binaries but only a small proportion of these will evolve into X-ray binaries.

Not all galactic X-ray sources are X-ray binaries. A few of them are young pulsars and some others are supernova remnants.

X-ray binaries are classified according to the nature of the companions to the compact object (the star from which it is taking material). If its mass is smaller (larger) than that of the Sun, they are called Low (High) Mass X-ray binaries.

In Low Mass systems, the companions are small reddish stars or even other degenerate stars, as in 4U1820-30, shown in Figure 4. The compact

object is much more massive than the companion and distorts its shape, stealing matter from it.

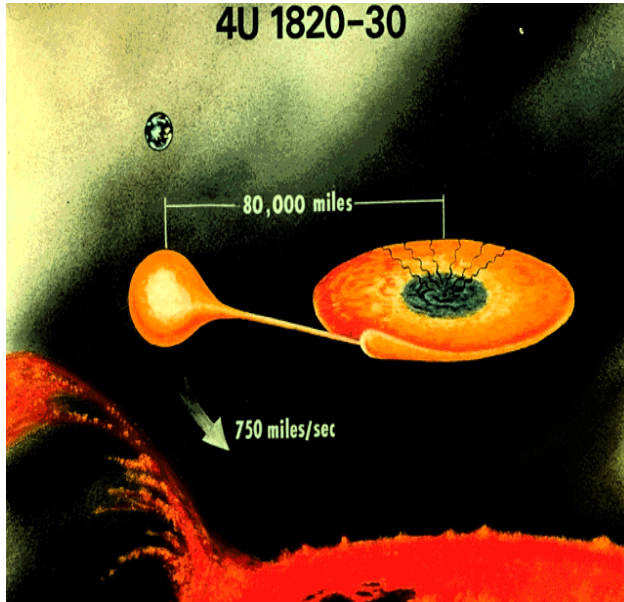
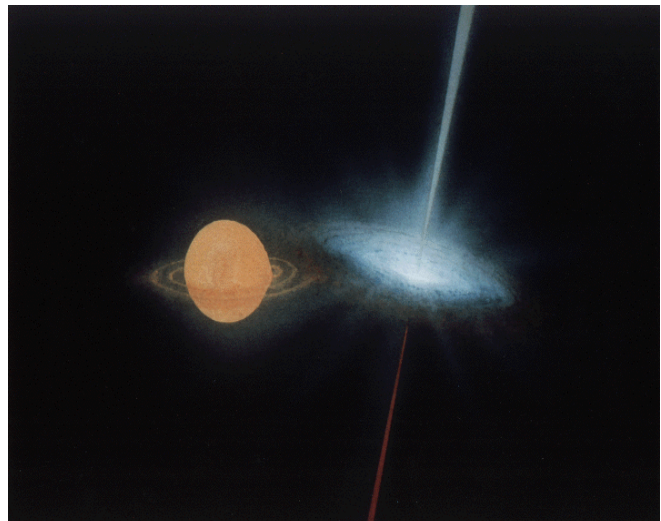


Figure 4: An artist's view of the Low Mass X-ray binary 4U 1820-30. A white dwarf (whose size is compared with that of the Earth) is being distorted by a neutron star and losing matter to it. The in-falling matter forms an accretion disc around the neutron star before being accreted. One can also compare the size of the objects with that of the Sun (a small part of which can be seen at the bottom). The neutron star at the center of the accretion disc is too small to be seen.

In High Mass systems, the companions are large, massive, blue stars with masses in the range 10-40 solar masses. Sometimes, the compact object in the binary is a neutron star with strong magnetic field (up to  $10^{12}$  G).

Figure 5: An artist view of the unusual High Mass X-ray Binary SS443. The supergiant star is losing mass to the neutron star (or black hole) companion, but the accretion disc is not stable. Particles are being accelerated at enormous speeds (up to  $1/3$  of the speed of light) and emitted in two jets that can be seen in the radio wavelengths.



When the matter that has been gravitationally captured by the neutron star (which is a high-temperature plasma, consisting of ionized atoms and free electrons) comes close, it is trapped by the magnetic field. From then on, it

can only move following the magnetic field lines. They take it to the magnetic poles of the neutron star. Since all the lines are converging there, the density is very large and the particles will be decelerated in a collisionless shock or will just crash against the neutron star surface. In both cases, they must release their energy in the form of X-rays that will have to make their way out the magnetic field in a narrow beam. In the same way as one sees radio pulses from an isolated pulsar, one now sees X ray pulses: one speaks of an X ray pulsar. High Mass X-ray Binaries (HMXRB) contain large blue stars (spectral types O and B) and a neutron star companion (in some occasions a black hole, as is the case of Cyg X--1, shown in Figure 6). The large blue stars are very bright: when observing the system in infrared, optical or ultraviolet, one sees only it. The neutron star can only be seen in the X-ray range. Most HMXRB are X-ray pulsars.



Figure 6: An artist impression of the High Mass X-ray Binary Cygnus X-1. The supergiant star HD226868 with about thirty solar masses, is being distorted by the presence of a black hole with a mass around 15 solar masses. There is an extremely hot accretion disc around the black hole where the X-rays are being produced.

When a star reaches the last stages of its life, after having consumed most of the hydrogen in its nucleus, the outer layers begin expanding and the star grows enormously. It becomes a supergiant. As it grows, the gravitational pull on its outer layers decreases. It is then when the gravitational attraction of an orbiting compact object in a close orbit can start distorting the shape of the supergiant and the dragging of matter towards the compact star begins.

As the supergiant expands, it increases in brightness. The outer layers of its atmosphere are continuously bombarded by very energetic photons. They push a stream of particles along with them. These particles dissipate into the empty space around the star at very high velocities. This is called a radiation-driven stellar wind. Sometimes, a neutron star in a rather distant orbit can pick up some of these particles and start the accretion process, becoming a weak X-ray source. However, if a neutron star is orbiting a star which has not reached the supergiant phase, it will not be able to steal any material from it and will not become an X-ray source.

### 3. The centre of the Milky Way

#### 3.1. Galactic Black holes: general features

For now a few years, we have known about the existence of a massive black hole (3 million solar masses) at the centre of our galaxy, the Milky Way. We briefly present below what we have learned of it. At the same time, evidence for the presence of very massive black holes at the centre of other nearby galaxies, such as Andromeda, has been obtained. It seems likely, today, that all galaxies should have a massive black hole in their centre. Indeed, evidence for the presence of very massive black holes at the centre of smaller groupings of stars has also been accumulated recently. As an example, such a black hole has been identified at the centre of the globular cluster  $\omega$  Cen with a mass of  $4 \pm 1 \cdot 10^4$  solar masses. The most massive black holes we know of take the form of quasars and their masses may reach several billion solar masses. One of the most famous is Cyg A, 200 Mpc away, which was discovered first as a very loud radio source. Such supermassive black holes are embedded in dense environments and accrete gigantic amounts of matter: one talks of active galactic nuclei. In active galactic nuclei, the horizon, 3 km/solar mass or better 10 light seconds per million solar masses, is surrounded by a very brilliant accretion disk made of high temperature plasma. Around it, at much larger distances, one finds a torus of gas and dust, or circumnuclear ring. Depending on where one looks from, it may obscure the accretion disk. Perpendicular to the accretion disk, namely parallel to the magnetic field which it contains, are two relativistic jets of electrons and possibly ionized nuclei. Both the jets and the accretion disk are the seat of intense synchrotron radiation with wave lengths extending from radio to X-rays. The more massive the active galactic nucleus the more marked are these features.



### 3.2. Sgr A\*



Figure 7: The Green bank radio telescope

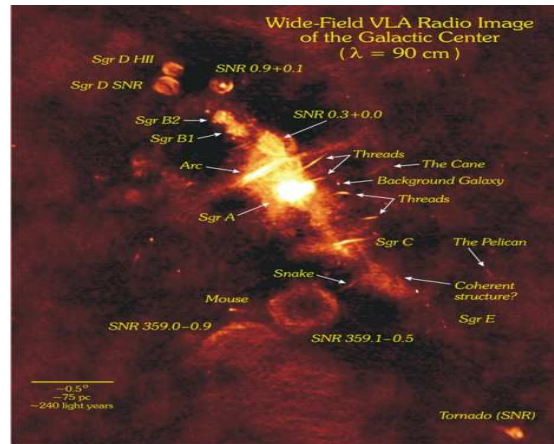


Figure 8: Broad 90cm VLA view of the centre of the Milky Way

The emission of radio waves from the centre of the Milky Way was first discovered in 1932 by Karl Jansky. It was only in 1974 that a point radio source, Sgr A\*, was resolved at Greenbank (Figure 7), very high resolution images of which are now available from GHz interferometry (Figures 8 and 9).

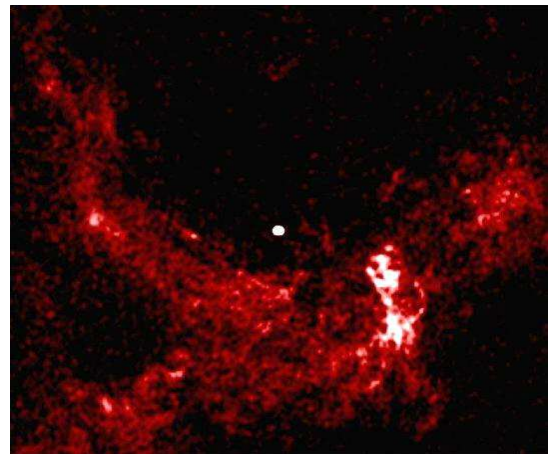
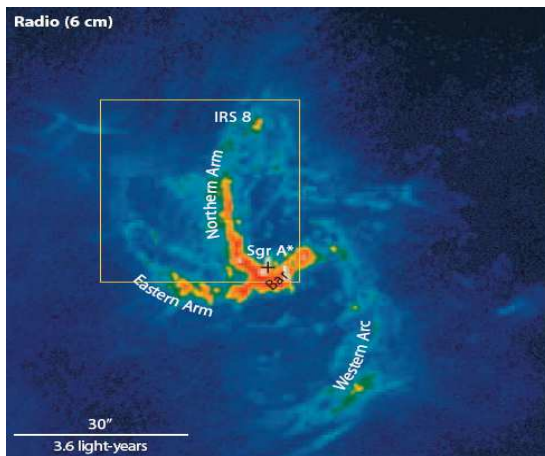


Figure 9: Left: Zooming in at 6 cm wave length. Many supernova remnants have been identified. Star density is one million times higher than near the Sun. Many SN explosions, dense star forming region. A three arm structure is revealed in Sgr A

Right: Highest resolution VLA image, 2ly×2ly. The bright spot is Sgr A\*.

The Very Large Base Array, which uses an Earth-size base, found that Sgr A\* is solidly anchored at the centre of the Galaxy, with a very small peculiar movement, in agreement with the idea that it grew from accreting material from the Galaxy.

Sgr A\* is not visible at optical wavelengths because the centre of the Milky Way is obscured by heavy clouds of dust. But at longer wave lengths, the dust becomes transparent: already in the near infrared one starts to see the region glowing (Figure 10) and the mid and far infrared reveal stars and allow studying their movement.

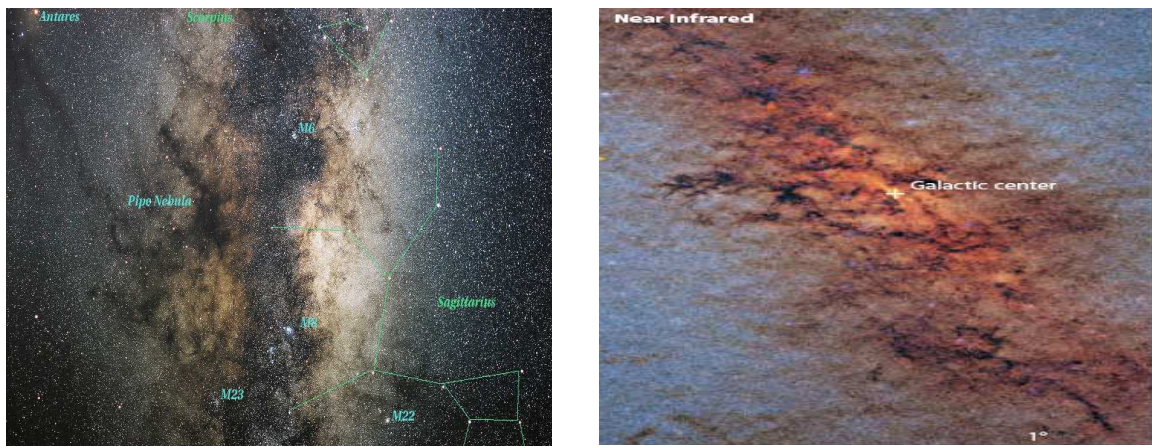


Figure 10: Large scale views of the centre of the Milky Way in the visible (left) and near infrared (right).

Indeed, the most spectacular achievement of infrared observations, made from ground using adaptative optics on the Very Large Telescope, was the study of the Kepler movement of stars around the black hole, in particular of a star having a very eccentric orbit with a period of 15.2 years (Figure 11), which measured the mass of the black hole at the level of three million solar masses.

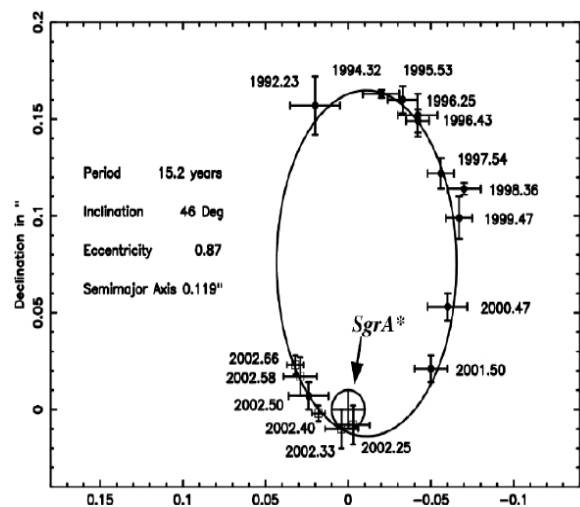
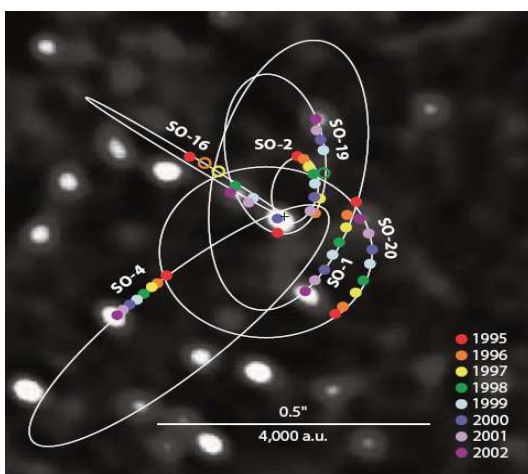
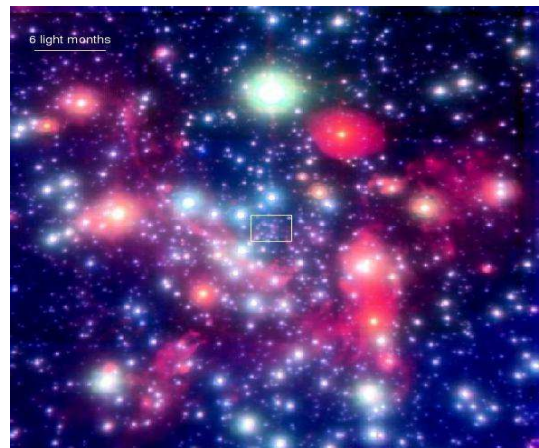
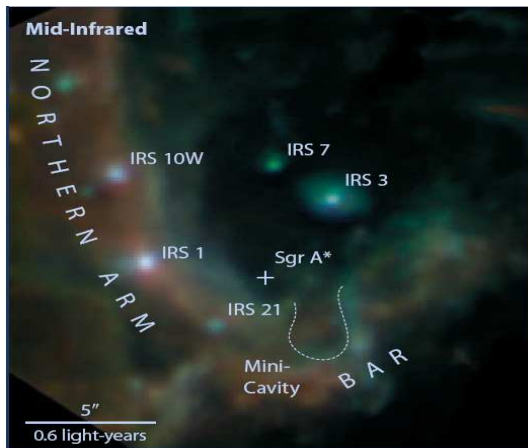


Figure 11: Zooming in (mid-infrared). Stars are observed in infrared as orbiting around a 3million solar masses black hole.

The region has also been intensively observed in X-rays and  $\gamma$  rays. Putting all these observations together has made it possible to draw a detailed picture of the centre of the Galaxy and to study Sgr A\* in much detail. As shown in Figure 12, the point radio source has an X-ray counterpart, and its diameter is smaller than 5 light minutes, a limit only 5 times as large as the Schwarzschild diameter of the black hole. The infrared counterpart is much fainter and was only discovered after having realized that it was occasionally flaring, while strong and clear flaring is detected in X-rays (Chandra) and accurately measured, confirming the very compact nature of the source. In addition, X-ray observations suggest the presence of a jet perpendicular to the

galactic plane, namely parallel to the Galaxy angular momentum, reinforcing the idea that Sgr A\* is solidly anchored to the Galaxy.

All observations provide evidence for a very high star density surrounding Sgr A\*, typically a million times higher than in the environment of the Sun. As a result, intense activity takes place, both in terms of star formation and in terms of supernova explosions, as testified by the high density of supernova remnants present in the region.

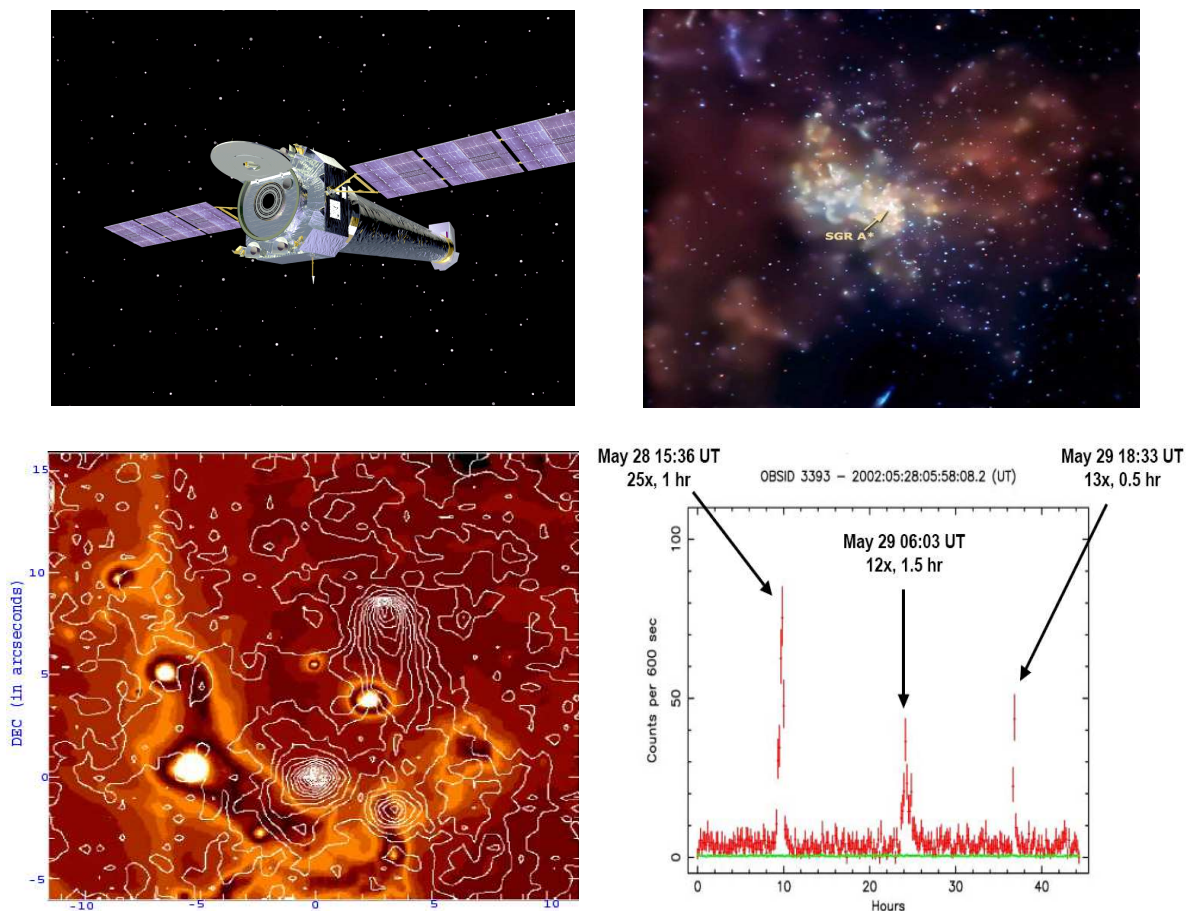


Figure12: Top left, CHANDRA, used to observe Sgr A\* in X rays; Top right, an X ray view of the galactic centre; Bottom, left, superposition of a 2-8 keV Chandra picture with Naos Conica VLT mid infrared; Sgr A\* source <1.4 arcsec in diameter, consistent with expected accretion disc of a 3 million solar masses black hole; Bottom right, observation of X ray flares.

Independent evidence is obtained from the high population of active X-ray binaries [1], twenty times higher than expected (Figure 13). These are black

holes accreting matter from their companion and their abnormal abundance is due to a high density of stellar black holes in the region: they interact with normal binaries by exchanging partner. It implies that a swarm of ten thousand or so stellar black holes are orbiting Sgr A\*. It is this observation which motivated the present study.

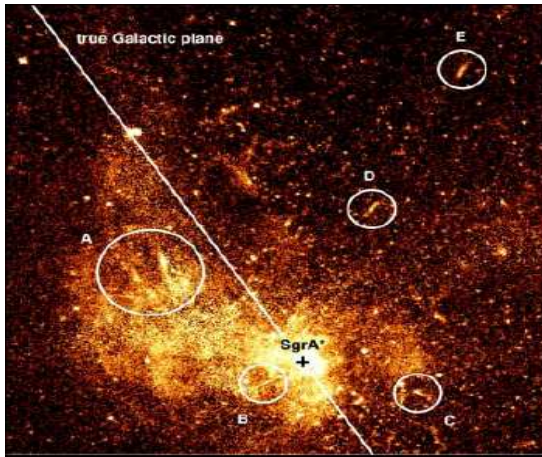


Figure 13: Twenty times as many active X ray binaries as expected, suggesting that ten thousand stellar black holes may be orbiting Sgr A\*.



Figure 14: A ring of dust (6.5ly radius) fed by dense clouds 25 to 50 ly away and three arms of hot gas ( $>10000\text{K}$ ) spiralling toward Sgr A\*.

Many other observations and measurements have revealed the structure of the immediate environment of Sgr A\*, all consistent with the black hole hypothesis. In particular (Figure 14), a ring of gas and dust of 1 to 2 pc radius has been shown to surround Sgr A\*. It is fed by dense clouds, 10 to 20 pc away; three arms of hot gas ( $>10^4\text{ K}$ ) spiral toward Sgr A\*.

While none of these observations can be taken as a strict proof that Sgr A\* is a black hole, it is their accumulation and their convergence that has convinced the astrophysics community that such is the case. Indeed, we do not know how to devise a crucial test that would unambiguously conclude that a celestial object is a black hole: most of its non trivial features occur beyond the horizon and are not accessible to us.

## 4. The three-body problem

### 4.1. History

The three-body problem considers three masses  $M_1$ ,  $M_2$ , and  $M_3$ , interacting mutually via Newton's law. In the restricted three-body problem,  $M_3$  is taken to be small enough so that it does not influence the motion of  $M_1$  and  $M_2$ , which are assumed to be in circular orbits about their center of mass. The orbits of three masses are further assumed to all lie in a common plane. If  $M_1$  and  $M_2$  are in elliptical instead of circular orbits, the problem is variously known as the “elliptic restricted problem” or “pseudorestricted problem”.

The efforts of many famous mathematicians have been devoted to this difficult problem, including Euler and Lagrange (1772), Jacobi (1836), Hill (1878), Poincaré (1899), Levi-Civita (1905), and Birkhoff (1915). In 1772, Euler first introduced a synodic (rotating) coordinate system. Jacobi (1836) subsequently discovered an integral of motion in this coordinate system (which he independently introduced) that is now known as the Jacobi integral. Hill (1878) used this integral to show that the Earth-Moon distance remains bounded from above for all time (assuming his model for the Sun-Earth-Moon system is valid), and Brown (1896) gave the most precise lunar theory of his time.

Poincaré, in 1899, emphasized qualitative aspects of celestial mechanics, including modern concepts such as phase space surfaces of section. Birkhoff (1915) further developed these qualitative methods. The important problem of regularization was considered by Thiele (1892), Painlevé (1897), Levi-Civita (1903), Burrau (1906), Sundman (1912), and Birkhoff (1915). Painlevé proved that all singularities are collisions for  $n = 3$ . Sundman found a uniformly convergent infinite series involving known functions that “solves” the restricted three-body problem in the whole plane

(once singularities are removed through the process of regularization). Since such global regularizations are available for this problem, the restricted problem of three bodies can be considered to be complete “solved”. However, this “solution” does not address issues of stability, allowed regions of motion, and so on, and so is of limited practical utility. Furthermore, an unreasonably large number of terms (of order  $10^{8'000'000}$ ) are required to attain the accuracy required for astronomical observations.

In physics and astronomy, Euler's three-body problem is to solve for the motion of a particle that is acted upon by the gravitational field of two other point masses that are either fixed in space or move in circular coplanar orbits about their center of mass. This problem is significant as an exactly soluble special case of the three-body problem, and an approximate solution for particles moving in the gravitational fields of prolate and oblate spheroids. This problem is named after Leonhard Euler, who discussed it in memoirs published in 1760 and showed that it had an exact solution. Joseph Louis Lagrange solved a generalized problem in which the centers exert both linear and inverse-square forces. Carl Gustav Jacob Jacobi showed that the rotation of the particle about the axis of the two fixed centers could be separated out, reducing the general three-dimensional problem to the planar problem.

By treating Euler's problem as a Liouville dynamical system, the exact solution can be expressed in terms of elliptic integrals. For convenience, the problem may also be solved by numerical methods.

#### ***4.2. Present approach***

In general, for  $N_{body}$  bodies in gravitational interaction, one can write Newton's law which gives the acceleration of body  $i$  as  $d^2x_i/dt^2 = \sum Gm_k(\mathbf{r}_k - \mathbf{r}_i)/(r_k - r_i)^3$  where  $G$  is Newton's gravity constant,  $m_i$  is the mass of body  $i$ ,  $\mathbf{r}_i$  the position vector of body  $i$  and  $t$  is the time. The sum extends over all bodies

(index  $k$ ) other than  $i$ . It is convenient to use units such that  $G=1$ ,  $\sum r_i=1$  and  $\sum m_i=1$ . Moreover, when describing a binary, it is useful to work in a frame in which the binary is initially at rest. Namely, at time 0,  $\sum m_i \mathbf{v}_i = \sum m_i \mathbf{r}_i = 0$  where we introduced velocities  $\mathbf{v}_i = d\mathbf{r}_i/dt$  and where the sum extends over the two members of the binary. Giving them indices 1 and 2, we have therefore at time zero  $r_1=m_2$  and  $r_2=m_1$ . In the case of a binary with circular orbits, the centrifugal acceleration balances the acceleration of gravity, namely the velocity obeys  $v_1^2/r_1 = Gm_2/(r_1+r_2) = m_2 = r_1$ , that is  $v_1=r_1$  and  $v_2=r_2$ .

As a general rule, we shall use throughout the units described above and work in the frame in which the binary is at rest at the origin of time. The initial conditions of the binary are then completely defined by the mass ratio of the stars in the binary, which sets their masses and original locations, and one of the velocity vectors, the other obeying relation  $m_1 \mathbf{v}_1 + m_2 \mathbf{v}_2 = 0$ . The initial parameters defining the third star (location, velocity and mass) can be chosen at will.

The simulation proceeds in small steps of time,  $\Delta t$ , each time calculating for each of the bodies the Newton's acceleration  $\gamma$  induced on it by the other bodies and modifying its position and velocity according to  $\mathbf{v}' = \mathbf{v} + \gamma \Delta t$  and  $\mathbf{x}' = \mathbf{x} + \mathbf{v} \Delta t + 1/2 \gamma \Delta t^2$ . For increased precision  $\gamma$  is calculated before and after the time interval  $\Delta t$  and the average of the two vectors is used to transform  $\mathbf{v}$  and  $\mathbf{x}$ .

In general, two bodies are bound if, in their centre of mass system, the total energy, potential plus kinetics, is negative. Otherwise they are unbound. In the case of the binary, as all variables are expressed in their centre of mass system, the binding condition reads simply  $E_{12} = 1/2 m_1 v_1^2 + 1/2 m_2 v_2^2 + m_1 m_2 < 0$ . Here  $E_K = 1/2 m_1 v_1^2 + 1/2 m_2 v_2^2$  is the kinetic energy and  $E_G = m_1 m_2$  is the gravity potential energy. In the case of a pair containing the third mass, say masses 1



and 3, the centre of mass has a position vector  $(m_1\mathbf{r}_1+m_3\mathbf{r}_3)/(m_1+m_3)$  and a velocity  $(m_1\mathbf{v}_1+m_3\mathbf{v}_3)/(m_1+m_3)$ . Hence the binding condition reads  $E_{13}=\frac{1}{2}m_1u_1^2+\frac{1}{2}m_3u_3^2+m_1m_3<0$  where  $\mathbf{u}_1=m_3(\mathbf{v}_1-\mathbf{v}_3)$  and  $\mathbf{u}_3=m_1(\mathbf{v}_3-\mathbf{v}_1)$ . The capture of a member of the binary, say mass 1, by the third mass is characterized by  $E_{12}$  changing from negative to positive while  $E_{13}$  changes from positive to negative.

## 5. The two body case

The present section concentrates on the two body case which is well known to obey Kepler's laws with elliptical, parabolic or hyperbolic orbits. It is used to validate the method.

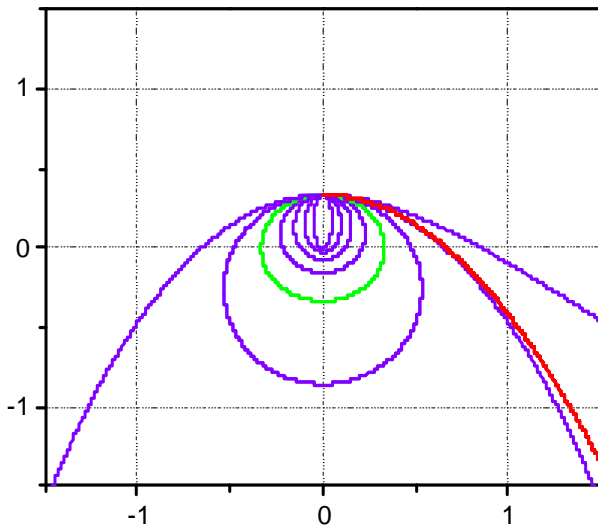


Figure 15: Trajectories of one of the stars of a binary for various values of the initial velocity (see text).

Figures 15 and 16 illustrate the case of a binary made of two stars of equal masses. In Figure 15 the initial velocities are taken perpendicular to the line joining the stars and the trajectories of one of the stars are shown for various values of the initial velocities  $v$ . In the particular case where  $v=r$  we find circular orbits as expected (green trajectory). The system is bound

and the gravitational energy is twice as large as the kinetic energy and negative. For smaller velocities, the system remains bound and the trajectories are ellipses having their minor axis parallel to the  $x$  axis. For larger velocities, the system remains bound until they become a factor  $\sqrt{2}$  larger than the circular velocity. Then the system gets unbound and the trajectory is a parabola (shown in red). For still higher velocities, the system remains unbound and the trajectories are hyperbolae.

In Figure 16, the initial velocities are taken of magnitudes  $v=r$  but the angle  $\theta$  they make with the  $x$  axis is varied. For  $\theta=0$  the trajectory is circular (shown in green). Here, contrary to the preceding case, the initial energy is always the same (the kinetic energy depends only on the modulus of the

velocity, not on its angle) and the system remains bound. This is illustrated in Figure 17 where the total energy,  $E_{12}$ , is shown as a function of  $v^2$ . The value  $-1/8$ , corresponding to the circular case (green point) and to the orbits shown in Figure 17, is indicated by a black line. The transition from bound to unbound ( $E_{12}=0$ ) occurs at  $v^2/r^2=2$  (red point). As expected,  $E_{12}=(v^2/r^2-2)/8$ .

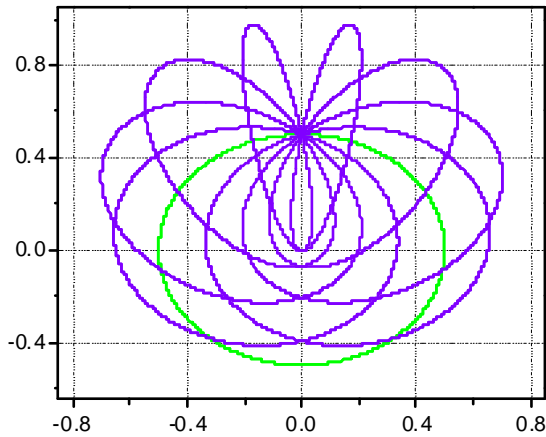


Figure 16: Trajectories of one of the stars of a binary for various angles of the initial velocity (see text).

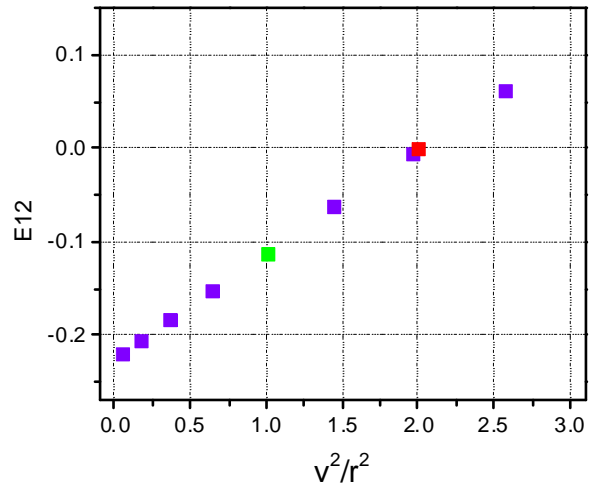


Figure 17: Dependence of the binary binding energy on initial velocity (see text)

When the two masses are unequal, the above results remain qualitatively the same. Figure 18 extends Figure 17 to unequal masses. The lines shown are for  $m_1=m_2$ ,  $m_1=2m_2$ ,  $m_1=5m_2$ ,  $m_1=10m_2$ ,  $m_1=100m_2$ . Note that for  $m_1=\lambda m_2$ , as  $m_1+m_2=1$ ,  $m_1 m_2 = \lambda/(1+\lambda)^2$ ,  $E_{12}=(1/2 v^2/r^2 - 1)\lambda/(1+\lambda)^2$ .

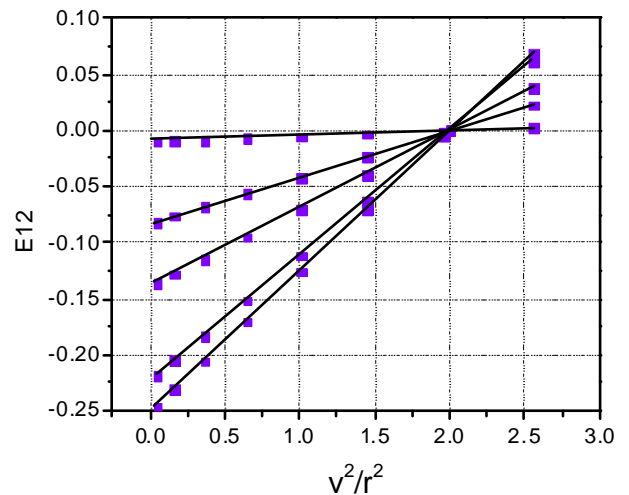


Figure 18: Dependence of the binary binding energy on initial velocity for various values of  $\lambda$  (see text)

Hence, for a same total mass, an asymmetric binary is less bound than a symmetric one and will be easier to tear apart when interacting with a third body.

Equal mass binaries with elliptic orbits are considered in Figure 19. Here,  $m_1=m_2=0.5$  and the initial velocities are parallel to the  $x$  axis and obey  $v_1/v_2=r_1/r_2$ , that is  $v_1=\lambda r_1$  and  $v_2=\lambda r_2$ . Orbits are shown for different values of  $\lambda$  and  $r_1=5r_2$ .

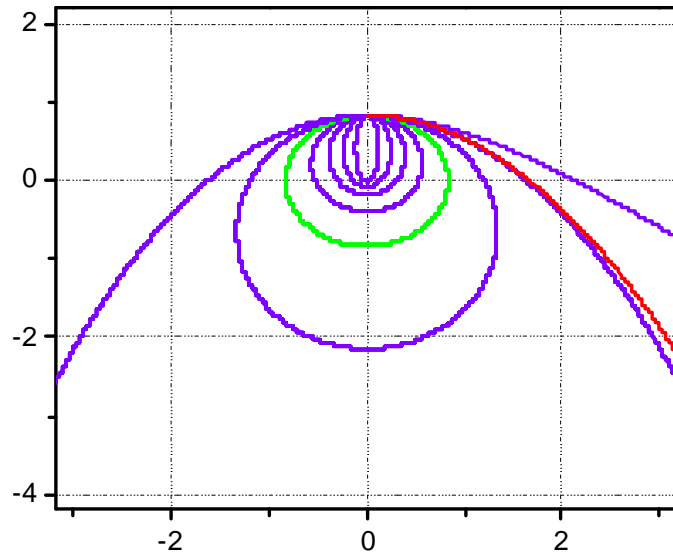


Figure 19: Trajectories of one of the stars of a binary for various of  $v/r$  (see text).

Here again the system evolves from a bound state when  $\lambda$  is small to an unbound state when  $\lambda$  is large. The values corresponding to a circular (green) and parabolic (red) trajectories are  $\lambda=1$  and  $\sqrt{2}$  respectively.

## 6. The three body case

### 6.1. General features

Here we consider the three body problem in the particular case where the initial state consists of a binary, namely a bound pair, and a more massive star far away from it, namely such that the three body system is globally unbound.. Two main evolutions are possible: either the binary and the massive star move away from each other with minimal disturbance to the binary or the massive star captures a member of the binary and moves away from the other, left alone, member of the binary. As the three body system is unbound in the initial state, it must remain so (conservation of energy) and a bound final state, with all three stars orbiting together on closed orbits, is excluded. However, on the contrary, a final state in which all stars are moving away from each other, namely where the action of the massive star has been to break the binary without capturing any of its members, is in principle possible.

We start this section by showing in Figures 20 to 22 three examples of the above evolution. Detailed descriptions of what is happening are given in the figure captions.

### 6.2. The capture cross-section: illustration on an example

In the present paragraph we study a three-body configuration system made of a binary on a circular orbit, the members of which have equal masses, and of a massive star moving toward it. The massive star has a mass equal to three times the mass of that of each star in the binary and is initially located at a distance equal to ten times the radius of the binary orbit. The trajectories are illustrated in the reference system in which the binary is originally at rest.

In Figure 23, we show a situation where the massive star is on the axis of the initial binary and moves toward it with a velocity equal to twice the initial velocities of the binary members. Note that if the binary were replaced by a single star having a mass equal to twice that of its members, the escape velocity would be  $\sqrt{8/5} \sim 1.26$  the initial velocity of the binary members. The system is found to evolve in two distinct phases. In a first phase (upper panels) the binary (1-red, 2-green) is strongly perturbed and nearly torn apart. It does manage to come back together, however, at the same time as the massive star (3-blue) arrives. What happens after this new encounter is that most of the momentum of the massive star is now transferred to the binary which moves on at high velocity away from the massive star. The orbits are now elliptical. The net result of the interaction is therefore a quasi-elastic collision between the massive star and the binary with only a small perturbation to the binary internal state. The lower panels of Figure 23 display the evolution of the kinetic and potential energies of the three-body and binary systems respectively. In the three-body case the first and second close encounters are seen as strong peaks in both kinetic and potential energies (which add up to a constant). In the second phase, the oscillations are associated with the binary orbital movement. In the binary case, similar features are observed; after the second close encounter, the total energy is less negative than it was at the very beginning, meaning that the binary is less closely bound in its current elliptical orbit than it was in its initial circular orbit.

The configuration of Figure 23 will now be used to study how it gets modified when the massive star starts moving to the binary away from the binary axis, either out of the binary plane or inside it. Moreover, the modifications induced by a change in the initial velocity of the massive star will also be studied. Our aim, in doing so, is to obtain an estimate of the

collision cross section, namely the effective interaction area offered by the binary to the massive star. What is meant here is that if the massive star points outside this area, the binary will remain bound while if it aims inside it will be torn apart, possibly resulting in a capture.

In a first step we study what happens when the initial position of the massive star is moved away from the binary axis, parallel to the plane of the binary, in steps of  $y$ . Up to  $y \sim 4.8$  orbit radii (o.r.), the massive star always captures one of the members of the binary. Usually, the capture occurs in a single go. However, in transition regions where the captured star switches from one to the other, a second (or more) close encounter occurs, reminiscent of the axial case of Figure 23. In practice, the red star is captured when  $y < \sim 2/3$  or  $y > \sim 3.9$  o.r. while the green star is captured when  $y$  lies between these two values. Examples are illustrated in Figure 24. The transition regions, with multiple encounters associated with alternating captures are very chaotic. In real situations of a dense environment, interactions with other additional nearby stars would very likely occur and complicate the picture.

In order to evaluate the range within which capture or break-up occurs, we define a collision cross-section,  $\sigma_c$ , as  $\sigma_c = \pi R_c^2$  where  $R_c$  is the collision radius defined as the average impact parameter (measured along  $y$  from the centre of the binary in the present cases) beyond which the binary is not torn apart, whether with or without capture. Figure 25 shows the dependence of  $R_c$  on the velocity  $V_3$  of the massive star in three different configurations: moving away in  $y$  from the binary axis parallel to the binary plane and moving away in  $y$  from the  $x$  axis in the binary plane in each of the positive and negative directions. The differences observed between the three configurations are the result of the dissymmetry introduced by the movement of rotation of the binary. At large values of  $V_3$ , the binary radius defines the

scale of the problem while at smaller values, there is sufficient time for the massive star to attract the binary in its neighborhood and interact with it.

In practical cases, we do not expect the initial relative velocity between the massive star and the binary to be significantly larger than the velocities of the binary members within the binary cms. In such cases, we see that large collision radii can be expected, most collisions resulting in capture. This implies large capture cross-sections in most practical cases. Figure 26 displays the dependence of  $R_c$  on  $V_3$  for three different values of the mass  $M_3$  of the massive star (2, 3 and 4 times the common mass of the binary members) and for each of the configurations in which the massive star is moved in  $y$  in the binary plane away from the  $x$  axis. At large values of  $V_3$  the collision radius is nearly independent on the mass of the massive star, confirming that the scale is uniquely defined by the size of the binary. At lower values of  $V_3$ , on the contrary, the collision radius depends on  $M_3$  approximately as  $M_3^{1/3}$  implying  $\sigma_c \sim M_3^{2/3}$ .



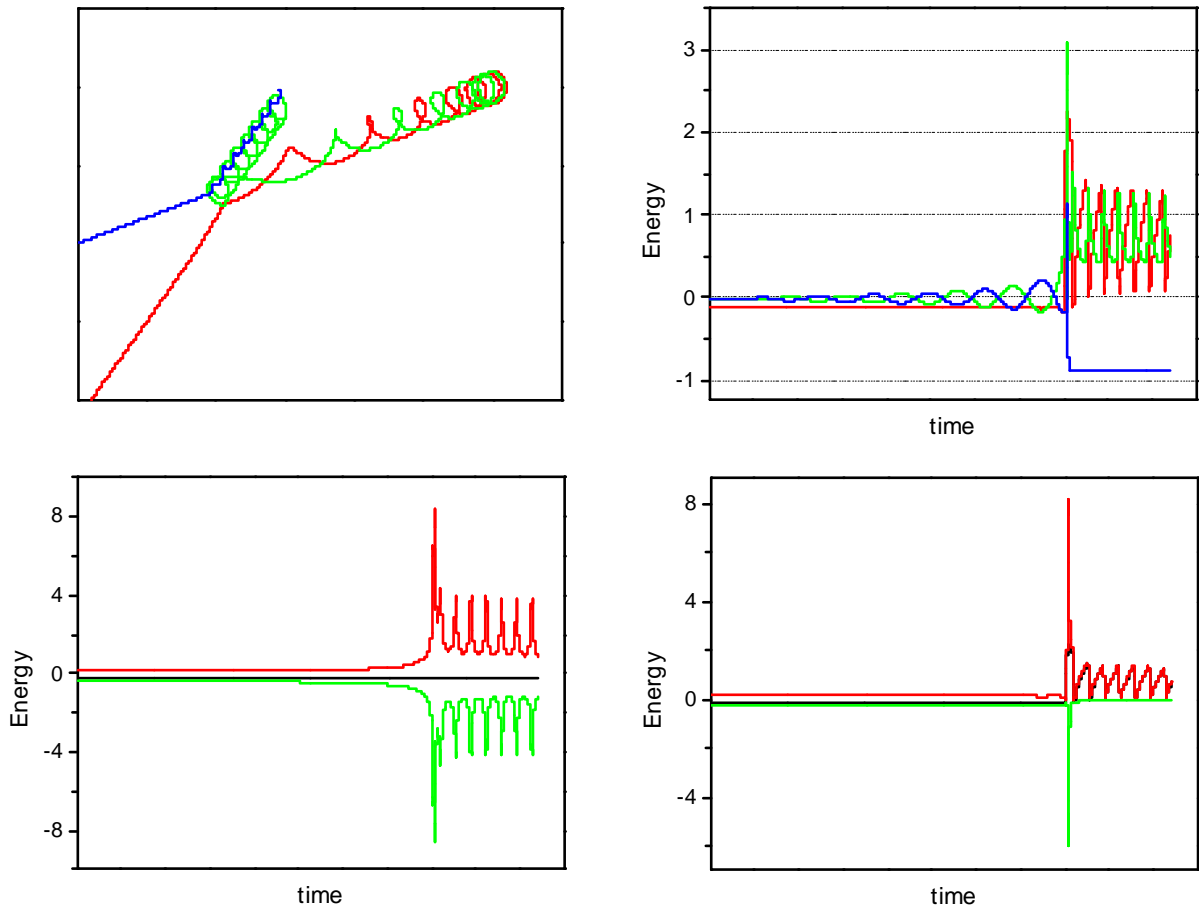


Figure 20: Example of a capture.

The trajectories are shown on the top left. All three stars are coplanar and remain so. The binary (nr 1, green and nr 2, red) starts from the right. It is made of two equal mass stars originally on circular orbits. The massive star (nr 3, blue, mass equal to 4 times the mass of the binary members) comes from the left and captures the green star, leaving the red star fly away alone.

The kinetic (red) and potential (green) energies of the three body system (bottom left) exactly compensate each other (black), as imposed by energy conservation. The total energy is negative.

The top right panel shows the pair total energies measured in the pair centre of mass frames. The energy of the 1-2 pair (red) starts negative (the binary being bound) and becomes positive after capture. Strong out of phase oscillations are seen before capture on the energy of the 1-3 (green) and 2-3 (blue) pairs. After capture, the energy of the 2-3 pair becomes negative and that of the 1-2 pair becomes positive, as expected. Here again the energies of the unbound pairs display strong out of phase oscillations.

The bottom right panel displays the sharing between potential (green) and kinetic (red) energies in the case of the 1-2 pair (in its centre of mass system). The total energy is shown in black. After capture, the potential energy of the pair quickly cancels (as the stars get far apart) while the kinetic energy keeps oscillating, a result of the orbiting of the captured green star around the blue star (remember that we are in the green-red cms).

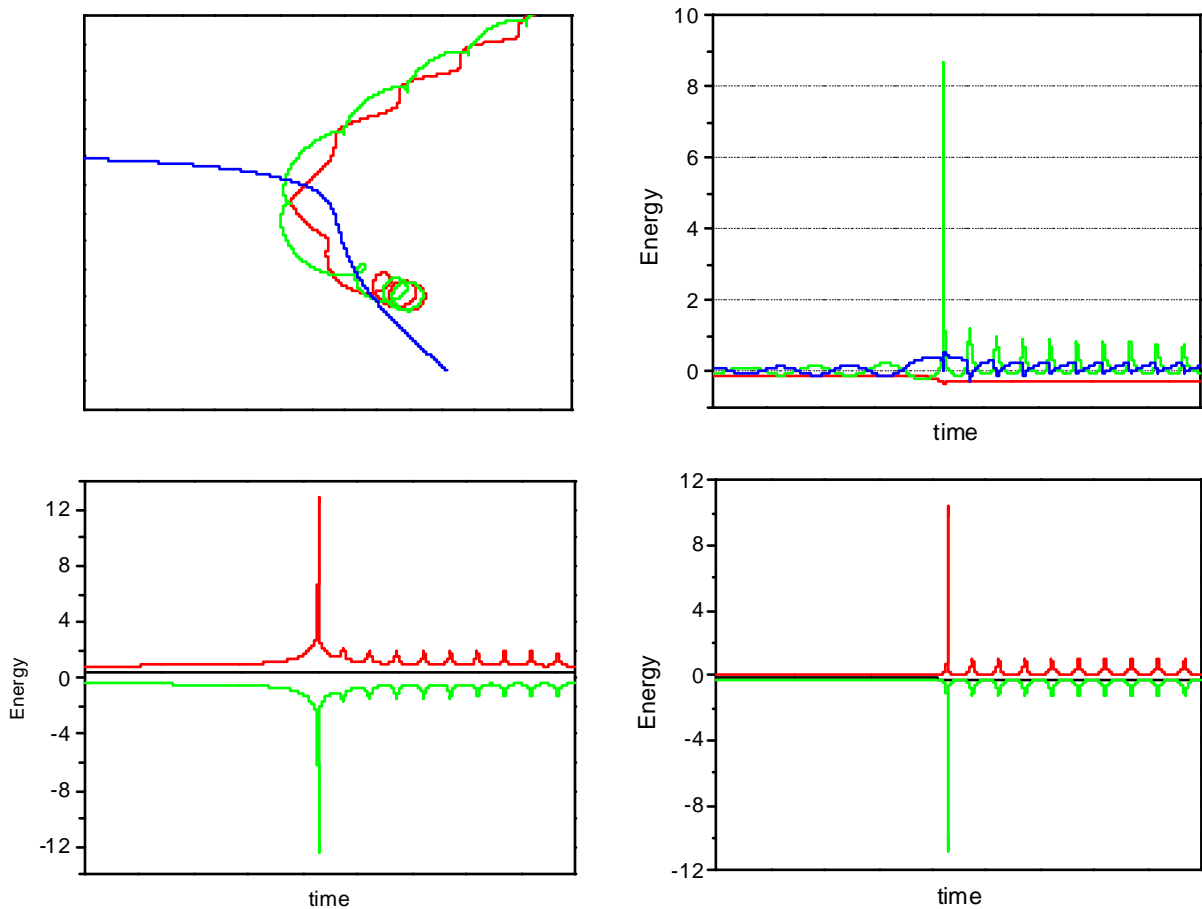


Figure 21: A case of no capture.

Top left: the trajectories are shown with the same conventions as in Figure 20. The red-green binary scatters against the massive blue star but the pair is not broken. The stars are coplanar and have the same masses as in Figure 20 with the binary initially on circular orbits.

Bottom left: kinetic and potential energies of the three body system. Before scattering, the binary is on circular orbits: its kinetic and potential energies are independently constant. After scattering, on the contrary, the binary has been perturbed and is on elliptical orbits with oscillations of its respective potential and kinetic energies.

Top right: the pair total energies in their cms. The binary (red) is more strongly bound after scattering than before. The oscillations seen in the unbound pairs are the result of the orbiting of the binary (they are measured in the cms of the unbound pairs).

Bottom right: binary kinetic and potential energies. After scattering, the orbits become elliptical, causing an oscillation of the sharing of the total energy between potential and kinetic.

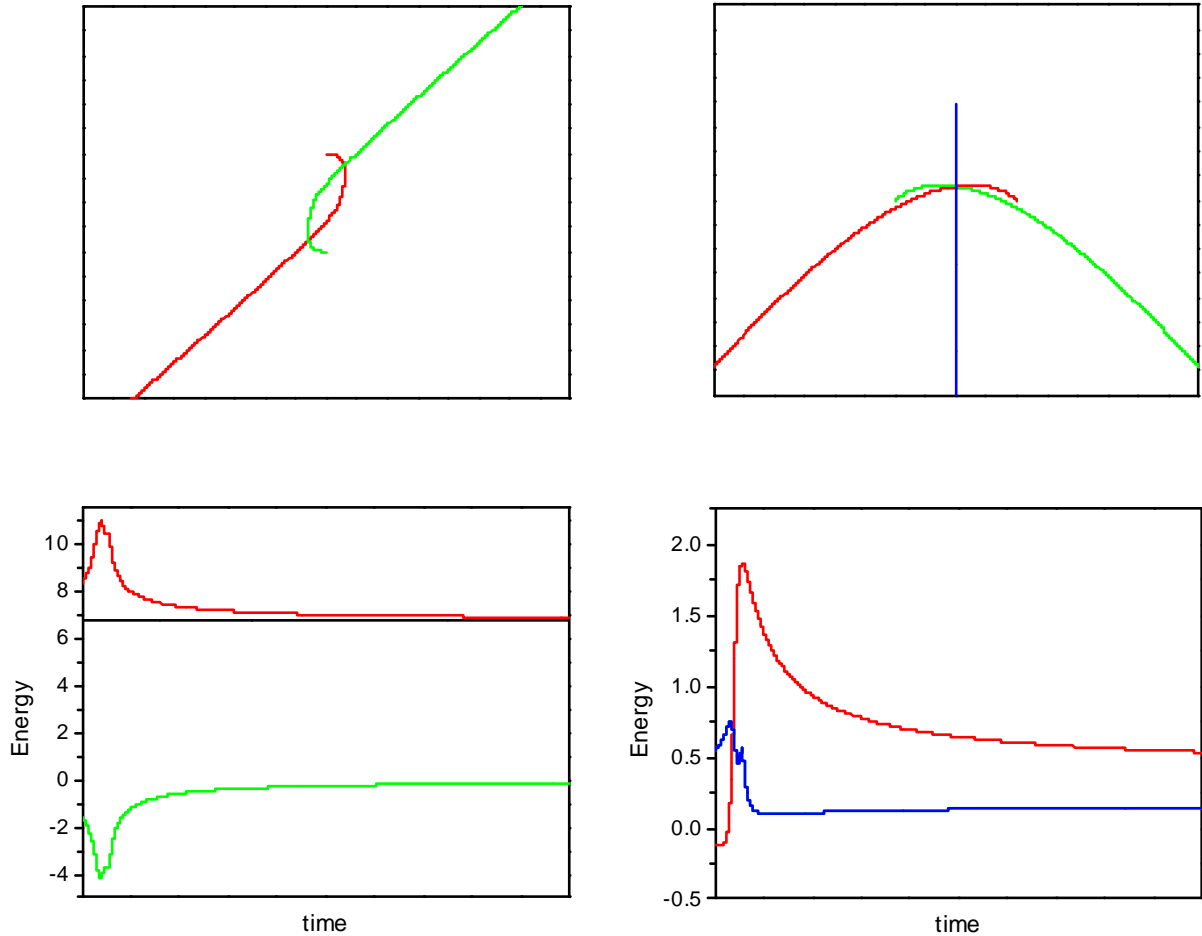


Figure 22: An example of break up.

The binary (green-red) is originally on a circular orbit in the  $x$ - $y$  plane. The massive star (blue, mass equal to three times the mass of each member of the binary) comes on a trajectory normal to the binary plane aiming at the centre of the binary orbit. The initial velocity of the blue star is 5 times as large as the initial velocities of the members of the binary.

Top left: trajectories in the  $x$ - $y$  plane (the blue star is at  $x=y=0$  all the time).

Top right: trajectories in the  $y$ - $z$  plane.

Bottom left: The total kinetic (red) and potential (green) energies of the three body system. The total energy (black) is of course constant and positive.

Bottom right: The total pair energies (kinetic + potential) for each of the three pairs (1-2 red, 1-3 and 2-3 blue) in their cms. When the 1-2 pair is broken its total energy switches from negative to positive.

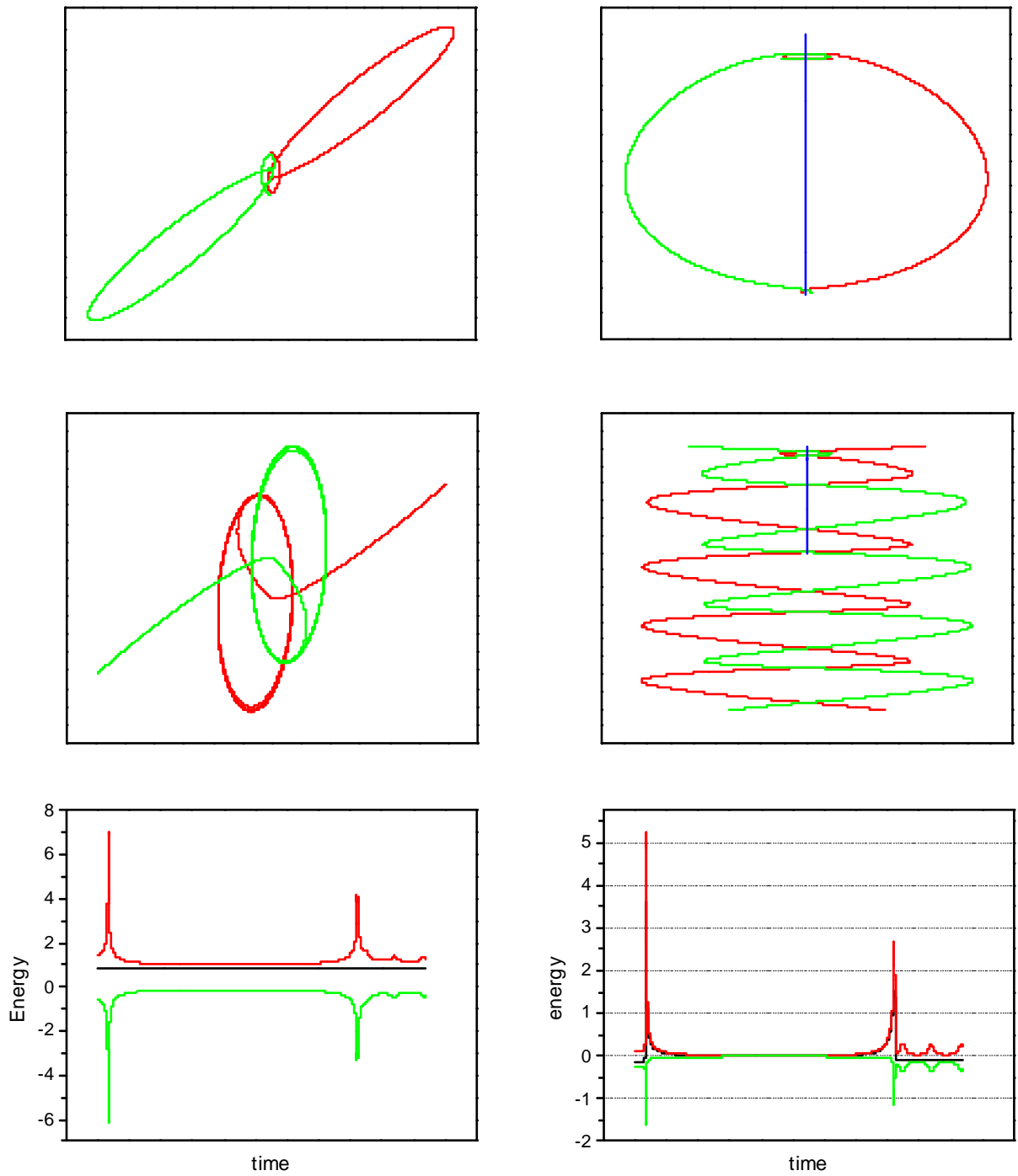


Figure 23: This case of a quasi-elastic collision proceeding in two distinct phases is described in the text. The upper panels are for the first phase and the middle panels for the second phase. The left panels are projections in the x-y plane and the right panels in the y-z plane. The lower panels display the sharing of energy between kinetic (red) and potential (green) for the 3-body (left) and binary (right) in their respective centre of mass systems.

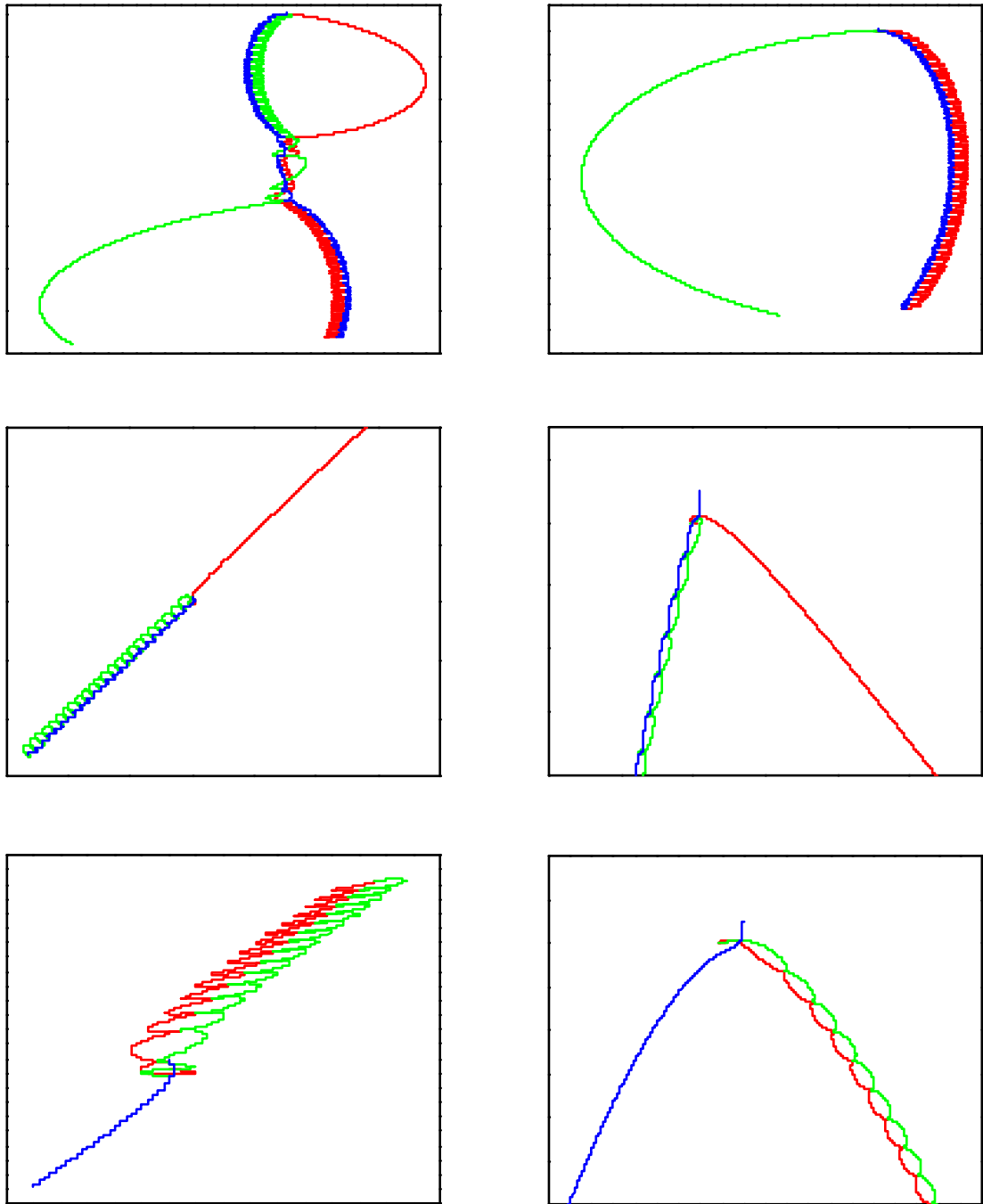


Figure 24: Moving away in  $y$  from the binary axis;  
 Upper panels: Examples of transition regions (y-z views). Left:  $y=3.76$  orbit radii. Right:  $y=0.034$  orbit radii.  
 Middle panels: Example of a clear capture,  $y=2$  orbit radii. Left: x-y view. Right: y-z view.  
 Lower panels: No capture,  $y=4.9$  orbit radii. Left: x-y view. Right: y-z view.

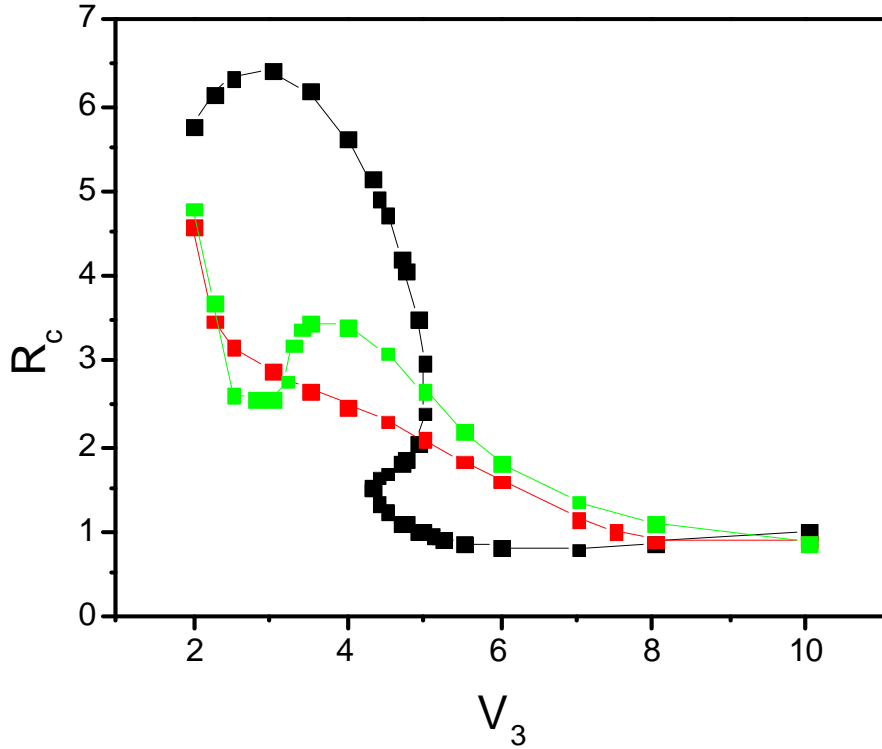


Figure 25: Dependence of the collision radius,  $R_c$ , on the initial velocity,  $V_3$ , of the massive star in three different configurations: moving away in  $y$  from the binary axis parallel to the binary plane (green) and moving away in  $y$  from the  $x$  axis in the binary plane in each of the positive (black) and negative (red) directions. The differences observed between the three configurations are the simple result of the dissymmetry introduced by the movement of rotation of the binary. Here, the velocity of the massive star is measured in units of the initial velocity of each of the binary members. Initially, the binary has circular orbits and its centre of gravity is at rest. The collision radius is measured in units of the radius of the initial binary orbit (o.r.). Initially, the massive star starts from a distance of 10 o.r. from the centre of the binary.

For large values of  $V_3$  the collision radius is essentially equal to the initial radius of the binary orbit. When the massive star hits the binary, it simply tears it apart; there is no time to capture one of the members. When the massive star misses the binary, it kicks the binary away without tearing it apart but disturbs its internal movement, transforming the circular orbits in elliptical orbits, the more so the smaller the impact parameter.

For smaller values of  $V_3$  the collision radius gets larger as there is now enough time for the massive star to attract the binary in its neighborhood and to either tear it apart or to capture one of its members. As was seen in the configuration of Figure 24 ( $V_3=2$ , green case in the present figure), most collisions result in a capture while at large values of  $V_3$  all collisions result in break-ups. In between, either capture or break-up may occur. Up to  $V_3=2$ , one has mostly capture while above  $V_3=5$  one has mostly break up. The separator between capture and break up occurs in the  $3 < V_3 < 5$  region and its detailed shape depends on the particular configuration (green, red or black).

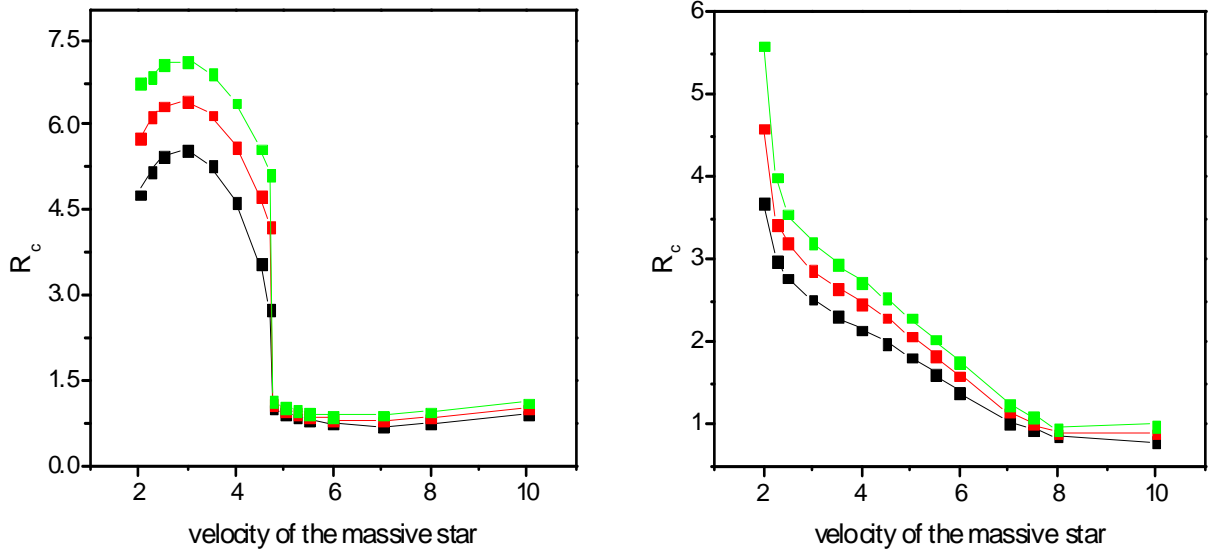


Figure 26: Dependence of the collision radius on the velocity  $V_3$  of the massive star for three different values of its mass:  $M_3=2$  (black), 3 (red) and 4 (green) times the common mass of the binary members. The left panel is for positive values of  $y$  and the right panel for negative values. In the large  $V_3$  region (break-up) the scale is independent from  $M_3$  and uniquely defined by the size of the binary. In the lower  $V_3$  region, the collision radius decreases with  $M_3$  approximately as  $M_3^{1/3}$ , implying a cross-section proportional to  $M_3^{2/3}$ .

## 7. Summary and conclusions

The present study has illustrated with numerous examples the phenomenon of capture which often takes place when a massive star approaches a binary. Depending on its impact parameter and kinetic energy, the massive star may capture one of the components of the binary and leave the other fly away alone. The notorious difficulty in solving the three-body problem analytically has been easily overcome using a very simple computer code. The complexity of the problem has been illustrated with examples displaying a strong chaoticity of the movement when very large perturbations happen to be induced. The concept of a collision cross-section has been introduced. At larger values of the relative velocity between the massive star and the binary, the cross-section is essentially equal to the area of the binary orbits and independent from the mass and initial kinetic energy of the massive star. In such cases, the binary is either torn apart (for impacts within the collision cross-section) or scattered away and perturbed in its internal movement for impacts outside the collision cross-section. At lower values of the relative velocity between the massive star and the binary, the cross-section is significantly larger than the area of the binary orbits. In such cases, the binary is torn apart and, in most cases, one of its members is captured by the massive star. The collision cross-section depends on the velocity of the massive star in a complicated way and is roughly proportional to  $M_3^{2/3}$ .

The importance of the capture phenomenon in astrophysics is particularly strong in dense environments such as globular clusters or the centre of galaxies. The case of the centre of the Milky Way has been discussed in some detail with a high density of X ray binaries suggesting the presence of many stellar black holes around Sgr A\*.



## References

1. M. P. Munro et al., *An overabundance of transient X ray binaries within 1 pc of the galactic centre*, arXiv:astro-ph/0412492 v1, 17 December, 2004 and references therein.
2. T. Alexander and M. Livio, *Orbital capture of stars by a massive black hole via exchanges with compact remnants*, arXiv:astro-ph/0403425 v2, 12 April, 2004 and references therein.
3. Kim Thi Phuong, *The black hole in the centre of the Milky Way*, Dissertation at the Hanoi University of Sciences, 2006.
4. Donat G. Wentzel, Nguyễn Quang Riệu, Phạm Viết Trinh, Nguyễn Đình Noãn, Nguyễn Đình Huân, *Thiên văn vật lý Astrophysics*, NXB Giáo dục, 2007.
5. [http://en.wikipedia.org/wiki/Binary\\_star](http://en.wikipedia.org/wiki/Binary_star).
6. [http://en.wikipedia.org/wiki/Three\\_body\\_problem](http://en.wikipedia.org/wiki/Three_body_problem).
7. <http://scienceworld.wolfram.com/physics/RestrictedThree-BodyProblem.html>.